Holography and Colliding Gravitational Shock Waves in Asymptotically AdS_5 Spacetime

Paul M. Chesler*
Department of Physics, MIT, Cambridge, Massachusetts 02139, USA

Laurence G. Yaffe†
Department of Physics, University of Washington, Seattle, Washington 98195, USA

(Received 22 November 2010; published 10 January 2011)

Using holography, we study the collision of planar shock waves in strongly coupled $\mathcal{N} = 4$ supersymmetric Yang-Mills theory. This requires the numerical solution of a dual gravitational initial value problem in asymptotically anti–de Sitter spacetime.

DOI: 10.1103/PhysRevLett.106.021601 PACS numbers: 11.25.Tq

Introduction.—The recognition that the quark-gluon plasma (QGP) produced in relativistic heavy ion collisions is strongly coupled [1], combined with the advent of gauge-gravity duality (or "holography") [2,3], has prompted much work exploring both equilibrium and nonequilibrium properties of strongly coupled $\mathcal{N} = 4$ supersymmetric Yang-Mills (SYM) theory, which may be viewed as a theoretically tractable toy model for real QGP. Multiple authors have discussed collisions of infinitely extended planar shock waves in SYM, which may be viewed as instructive caricatures of collisions of large, highly Lorentz-contracted nuclei. In the dual description of strongly coupled (and large N_c) SYM, this becomes a problem of colliding gravitational shock waves in asymptotically anti–de Sitter (AdS_5) spacetime. Previous work has examined qualitative properties and trapped surfaces [4–7], possible early time behavior [8–10], and expected late time asymptotics [11,12]. As no analytic solution is known for this gravitational problem, solving the gravitational initial value problem numerically is the only way to obtain quantitative results which properly connect early and late time behavior. In this Letter, we report the results of such a calculation, and examine the evolution of the post-collision stress-energy tensor.

Unlike previous work considering singular shocks with vanishing thickness [5,9], or shocks driven by nonvanishing sources in the bulk [5,6], we choose to study planar gravitational "shocks" which are regular, nonsingular, sourceless solutions to Einstein's equations. Equivalently, we study the evolution of initial states in SYM with finite energy density concentrated on two planar sheets of finite thickness (and Gaussian profile), propagating toward each other at the speed of light. The dual description only involves gravity in asymptotically AdS_5 spacetime; the complementary 5D internal manifold plays no role and may be ignored. Consequently, our results apply to all strongly coupled 4D conformal gauge theories with a pure gravitational dual description.

Gravitational description.—Diffeomorphism invariance plus translation invariance in two spatial directions allows one to write the 5D spacetime metric in the form

$$ds^2 = -A dv^2 + \Sigma^2[e^B d\boldsymbol{x}_\perp^2 + e^{-2B} dz^2] + 2dv(dr + F dz), \tag{1}$$

where A, B, Σ, and F are all functions of the bulk radial coordinate r, time v, and longitudinal coordinate z. We employ generalized infalling Eddington-Finkelstein coordinates. Lines along which all coordinates except r are constant are infalling radial null geodesics; the radial coordinate r is an affine parameter along these geodesics. At the boundary, located at $r = \infty$, v coincides with time in the dual quantum field theory. The geometry in the bulk at $v \geq 0$ is the causal future of $v = 0$ on the boundary. The ansatz (1) is invariant under the residual diffeomorphism $r \to r + \xi$, with ξ an arbitrary function of v and z.

For a metric of the form (1), Einstein's equations (with cosmological constant $\Lambda \equiv -6$) imply

$$0 = \Sigma'' + \tfrac{1}{2}(B')^2\Sigma, \tag{2a}$$

$$0 = \Sigma^2[F'' - 2(d_3B)' - 3B'd_3B] + 4\Sigma' d_3\Sigma, \quad -\Sigma[3\Sigma' F' + 4(d_3\Sigma)' + 6B' d_3\Sigma], \tag{2b}$$

$$0 = \Sigma^4[A'' + 3B' d_+B + 4] - 12\Sigma^2\Sigma' d_+\Sigma + e^{2B}\{\Sigma^2[\tfrac{1}{2}(F')^2 - \tfrac{7}{2}(d_3B)^2 - 2d_3^2B] + 2(d_3\Sigma)^2 - 4\Sigma[2(d_3B)d_3\Sigma + d_3^2\Sigma]\}, \tag{2c}$$

$$0 = 6\Sigma^3(d_+\Sigma)' + 12\Sigma^2(\Sigma' d_+\Sigma - \Sigma^2) - e^{2B}\{2(d_3\Sigma)^2 + \Sigma^2[\tfrac{1}{2}(F')^2 + (d_3F)' + 2F' d_3B - \tfrac{7}{2}(d_3B)^2 - 2d_3^2B] + \Sigma[(F' - 8d_3B)d_3\Sigma - 4d_3^2\Sigma]\}. \tag{2d}$$

$$0 = 6\Sigma^4(d_+B)' + 9\Sigma^3(\Sigma' d_+B + B' d_+\Sigma) + e^{2B}\{\Sigma^2[(F')^2 + 2(d_3F)' + F' d_3B - (d_3B)^2 - d_3^2B] + 4(d_3\Sigma)^2 - \Sigma[(4F' + d_3B)d_3\Sigma + 2d_3^2\Sigma]\}, \tag{2e}$$

$$0 = 6\Sigma^2 d_+^2\Sigma - 3\Sigma^2 A' d_+\Sigma + 3\Sigma^3 (d_+B)^2 - e^{2B}\{(d_3\Sigma + 2\Sigma d_3 B)(2d_+F + d_3A) + \Sigma[2d_3(d_+F) + d_3^2 A]\}, \tag{2f}$$

$$0 = \Sigma[2d_+(d_3\Sigma) + 2d_3(d_+\Sigma) + 3F' d_+\Sigma] + \Sigma^2[d_+(F') + d_3(A') + 4d_3(d_+B) - 2d_+(d_3B)] + 3\Sigma(\Sigma d_3 B + 2d_3\Sigma)d_+B - 4(d_3\Sigma)d_+\Sigma, \tag{2g}$$

where, for any function $h(v, z, r)$, $h' \equiv \partial_r h$ and

$$d_+h \equiv \partial_v h + \tfrac{1}{2}A\partial_r h, \qquad d_3 h \equiv \partial_z h - F\partial_r h. \tag{3}$$

Note that h' is a directional derivative along infalling radial null geodesics, d_+h is a derivative along outgoing radial null geodesics, and d_3h is a derivative in the longitudinal direction orthogonal to both radial geodesics.

Near the boundary, Einstein's equations may be solved with a power series in r. Solutions with flat Minkowski boundary geometry have the form

$$A = r^2\left[1 + \frac{2\xi}{r} + \frac{\xi^2 - 2\partial_v\xi}{r^2} + \frac{a_4}{r^4} + O(r^{-5})\right], \tag{4a}$$

$$F = \partial_z\xi + \frac{f_2}{r^2} + O(r^{-3}). \tag{4b}$$

$$B = \frac{b_4}{r^4} + O(r^{-5}), \tag{4c}$$

$$\Sigma = r + \xi + O(r^{-7}), \tag{4d}$$

The coefficient ξ is a gauge dependent parameter which encodes the residual diffeomorphism invariance of the metric. The coefficients a_4, b_4, and f_2 are sensitive to the entire bulk geometry, but must satisfy

$$\partial_v a_4 = -\tfrac{4}{3}\partial_z f_2, \qquad \partial_v f_2 = -\partial_z(\tfrac{1}{4}a_4 + 2b_4). \tag{5}$$

These coefficients contain the information which, under the holographic mapping of gauge/gravity duality, determines the field theory stress-energy tensor $T^{\mu\nu}$ [13]. Defining $\mathcal{E} \equiv \frac{2\pi^2}{N_c^2}T^{00}$, $\mathcal{P}_\perp \equiv \frac{2\pi^2}{N_c^2}T^{\perp\perp}$, $\mathcal{S} \equiv \frac{2\pi^2}{N_c^2}T^{0z}$, and $\mathcal{P}_\parallel \equiv \frac{2\pi^2}{N_c^2}T^{zz}$, one finds

$$\mathcal{E} = -\tfrac{3}{4}a_4, \qquad \mathcal{P}_\perp = -\tfrac{1}{4}a_4 + b_4, \tag{6a}$$

$$\mathcal{S} = -f_2, \qquad \mathcal{P}_\parallel = -\tfrac{1}{4}a_4 - 2b_4. \tag{6b}$$

Equations (5) and (6) imply $\partial_\mu T^{\mu\nu} = 0$ and $T^\mu_\mu = 0$.

Numerics overview.—Our Eqs. (2) have a natural nested linear structure which is extremely helpful in solving for the fields and their time derivatives on each $v =$ const null slice. Given B, Eq. (2a) may be integrated in r to find Σ. With B and Σ known, Eq. (2b) may be integrated to find F. With B, Σ and F known, Eq. (2d) may be integrated to find $d_+\Sigma$. With B, Σ, F and $d_+\Sigma$ known, Eq. (2e) may be integrated to find d_+B. Last, with B, Σ, F, $d_+\Sigma$ and d_+B known, Eq. (2c) may be integrated to find A. At this point, one can compute the field velocity $\partial_v B = d_+B - \frac{1}{2}AB'$, evolve B forward in time to the next time step, and repeat the process.

In this scheme, each nested equation is a linear ODE for the field being determined, and may be integrated in r at fixed v and z. The requisite radial boundary conditions follow from the asymptotic expansions (4). Consequently, the initial data required to solve Einstein's equations consist of the function B plus the expansion coefficients a_4 and f_2—all specified at some constant v—and the gauge parameter ξ specified at all times. Values of a_4 and f_2 on future time slices, needed as boundary conditions for the radial equations, are determined by integrating the continuity relations (5) forward in time.

Equations (2f) and (2g) are only needed when deriving the series expansions (4) and the continuity conditions (5). In this scheme, they are effectively implemented as boundary conditions. Indeed, the Bianchi identities imply that Eqs. (2f) and (2g) are boundary constraints; if they hold at one value of r then the other Einstein equations guarantee that they hold at all values of r.

An important practical matter is fixing the computational domain in r. If an event horizon exists, then one may excise the geometry inside the horizon, as this region is causally disconnected from the outside geometry. Moreover, one *must* excise the geometry to avoid singularities behind the horizon [14]. To perform the excision, we identify the location of an apparent horizon (an outermost marginally trapped surface) which, if it exists, must lie inside an event horizon [15]. For the initial conditions discussed in the next section, the apparent horizon always exists—even before the collision—and has the topology of a plane. Hence, one may fix the residual diffeomorphism invariance by requiring the apparent horizon position to lie at a fixed radial position, $r = 1$. The defining conditions for the apparent horizon then imply that fields at $r = 1$ must satisfy

$$0 = 3\Sigma^2 d_+\Sigma - \partial_z(F\Sigma e^{2B}) + \tfrac{3}{2}F^2\Sigma' e^{2B}, \tag{7}$$

which is implemented as a boundary condition to determine ξ and its evolution. Horizon excision is performed by restricting the computational domain to $r \in [1, \infty]$.

Another issue is the presence of a singular point at $r = \infty$ in the Eqs. (2). To handle this, we discretize Einstein's equations using pseudospectral methods [16]. We represent the radial dependence of all functions as a series in Chebyshev polynomials and the z dependence as a Fourier series, so the z direction is periodically compactified. With these basis functions, the computational domain may extend all the way to $r = \infty$, where boundary conditions can be directly imposed.

Initial data.—We want our initial data to describe two well-separated planar shocks, with finite thickness and energy density, moving toward each other. In Fefferman-Graham coordinates, an analytic solution describing a single planar shock moving in the $\mp z$ direction may be easily found and reads [11],

$$ds^2 = r^2[-dx_+dx_- + d\boldsymbol{x}_\perp^2] + \frac{1}{r^2}[dr^2 + h(x_\pm)dx_\pm^2], \quad (8)$$

with $x_\pm \equiv t \pm z$, and h an arbitrary function which we choose to be a Gaussian with width w and amplitude μ^3,

$$h(x_\pm) \equiv \mu^3(2\pi w^2)^{-1/2}e^{-(1/2)x_\pm^2/w^2}. \quad (9)$$

The energy per unit area of the shock is $\mu^3(N_c^2/2\pi^2)$. If the shock profile h has compact support, then a superposition of right and left moving shocks solves Einstein's equations at early times when the incoming shocks have disjoint support. Although this is not exactly true for our Gaussian profiles, the residual error in Einstein's equations is negligible when the separation of the incoming shocks is more than a few times the shock width.

To find the initial data relevant for our metric ansatz (1), we solve (numerically) for the diffeomorphism transforming the single shock metric (8) from Fefferman-Graham to Eddington-Finkelstein coordinates. In particular, we compute the anisotropy function $B_\pm$ for each shock and sum the result, $B = B_+ + B_-$. We choose the initial time v_0 so the incoming shocks are well separated and the $B_\pm$ negligibly overlap above the apparent horizon. The functions a_4 and f_2 may be found analytically,

$$\begin{aligned} a_4 &= -\tfrac{4}{3}[h(v_0 + z) + h(v_0 - z)], \\ f_2 &= h(v_0 + z) - h(v_0 - z). \end{aligned} \quad (10)$$

A complication with this initial data is that the metric functions A and F become very large deep in the bulk, degrading convergence of their spectral representations. To ameliorate the problem, we slightly modify the initial data, subtracting from a_4 a small positive constant δ. This introduces a small background energy density in the dual quantum theory. Increasing δ causes the regions with rapid variations in the metric to be pushed inside the apparent horizon, out of the computational domain.

We chose a width $w = 0.75/\mu$ for our shocks. The initial separation of the shocks is $\Delta z = 6.2/\mu$. We chose $\delta = 0.014\mu^4$, corresponding to a background energy density 50 times smaller than the peak energy density of the shocks. We evolve the system for a total time equal to the inverse of the temperature associated with the background energy density, $T_{\rm bkgd} = 0.11\mu$.

Results and discussion.—Figure 1 shows the energy density $\mathcal{E}$ as a function of time v and longitudinal position z. On the left, one sees two incoming shocks propagating toward each other at the speed of light. After the collision, centered on $v = 0$, energy is deposited throughout the region between the two receding energy density maxima. The energy density after the collision does not resemble the superposition of two unmodified shocks, separating at the speed of light, plus small corrections. In particular, the two receding maxima are moving outwards at less than the speed of light. To elaborate on this point, Fig. 2 shows a contour plot of the energy flux $\mathcal{S}$ for positive v and z. The dashed curve shows the location of the maximum of the energy flux. The inverse slope of this curve, equal to the outward speed of the maximum, is $V = 0.86$ at late times. The solid line shows the point beyond which $\mathcal{S}/\mu^4 < 10^{-4}$, and has slope 1. Evidently, the leading disturbance from the collision moves outwards at the speed of light, but the maxima in $\mathcal{E}$ and $\mathcal{S}$ move significantly slower.

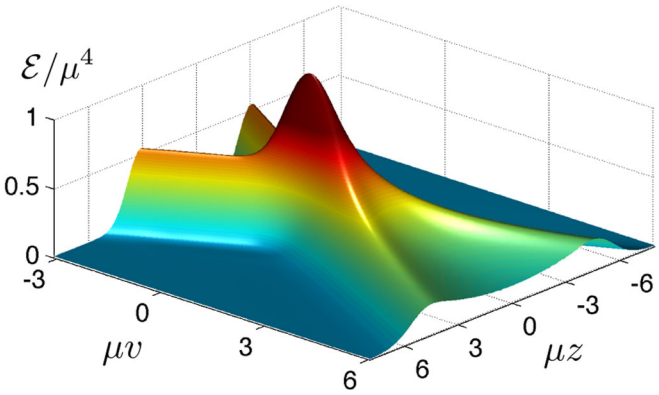

FIG. 1 (color online). Energy density $\mathcal{E}/\mu^4$ as a function of time v and longitudinal coordinate z.

Figure 3 plots the transverse and longitudinal pressures at $z = 0$ and $z = 3/\mu$, as a function of time. At $z = 0$, the pressures increase dramatically during the collision, resulting in a system which is very anisotropic and far from equilibrium. At $v = -0.23/\mu$, where $\mathcal{P}_\parallel$ has its maximum, it is roughly 5 times larger than $\mathcal{P}_\perp$. At late times, the pressures asymptotically approach each other. At $z = 3/\mu$, the outgoing maximum in the energy density is located near $v = 4/\mu$. There, $\mathcal{P}_\parallel$ is more than 3 times larger than $\mathcal{P}_\perp$.

The fluid-gravity correspondence [17] implies that at sufficiently late times the evolution of $T^{\mu\nu}$ will be described by hydrodynamics. To test the validly of hydrodynamics, Fig. 3 also plots (as dashed lines) the pressures $\mathcal{P}_\perp^{\rm hydro}$ and $\mathcal{P}_\parallel^{\rm hydro}$ predicted by the first-order viscous hydrodynamic constitutive relations [18]. At $z = 0$ the hydrodynamic constitutive relations hold within 15% at time $v_{\rm hydro} = 2.4/\mu$, with improving accuracy thereafter. At $z = 3/\mu$, they hold within 15% or better accuracy after $v_{\rm hydro} = 2.1/\mu$.

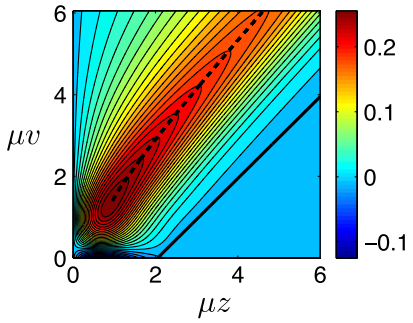

FIG. 2 (color online). Energy flux $\mathcal{S}/\mu^4$ as a function of time v and longitudinal coordinate z.

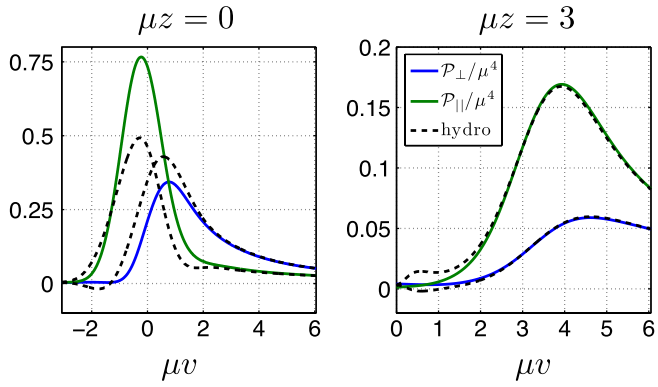

FIG. 3 (color online). Longitudinal and transverse pressure as a function of time v, at $z = 0$ and $z = 3/\mu$. Also shown for comparison are the pressures predicted by the viscous hydrodynamic constitutive relations.

At $z = 0$, where the flux $\mathcal{S} = 0$, the constitutive relations imply that the difference between $\mathcal{P}_\perp^{\text{hydro}}$ and $\mathcal{P}_{||}^{\text{hydro}}$ is purely due to viscous effects. Figure 3 shows that there is a large difference between $\mathcal{P}_\perp$ and $\mathcal{P}_{||}$ when hydrodynamics first becomes applicable, implying that viscous effects are substantial.

We have also examined the influence of second-order corrections in the hydrodynamic constitutive relations. At $z = 0$, the second-order corrections only change v_{hydro} by about 1%, whereas at $z = 3/\mu$ their addition *increases* v_{hydro} by 20%. Evidently, in front of the receding maxima in $\mathcal{E}$ and $\mathcal{S}$, second-order corrections are large, the system is still far from equilibrium, and agreement with the first-order constitutive relation is largely fortuitous.

Hydrodynamic simulations of heavy ion collisions at RHIC suggest that the produced QGP thermalizes in a time perhaps shorter than 1 fm/c [19]. Crudely modeling the boosted gold nuclei by our translationally invariant Gaussian shocks, for RHIC energies we estimate $\mu \sim 2.3$ GeV. Our results from Fig. 3 then imply that the total time required for apparent thermalization, from when the Gaussian shocks start to overlap significantly to the onset of validity of hydrodynamics, is $\Delta v_{\text{tot}} \sim 4/\mu \sim 0.35$ fm/c. Similar results for far-from-equilibrium relaxation times in SYM were also reported in Ref. [20].

We conclude by discussing the effect of the background energy density on our results. In the absence of a collision, the presence of the background energy density will cause a propagating shock to slowly attenuate in amplitude and eventually thermalize. We have computed single shock propagation with the background energy density used above, and found that the shock attenuates in amplitude by 2.5% in a time $\Delta v = 1/T_{\text{bkgd}}$. We have also studied the effect of increasing or decreasing the background energy density by a factor of 1.5. This results in a spacetime dependent $O(\delta)$ change in the stress tensor and perturbs the thermalization time v_{hydro} (at $z = 0$) by 1%. Lastly, we have also studied an expanding sheet of plasma which is initially localized at $z = 0$ and surrounded by vacuum. The initial conditions consisted of $B = 0$, a Gaussian profile in the energy density, and vanishing energy flux. At late times the stress has two outward moving maxima, just as it does for the colliding shocks. Furthermore, the tails in the stress move outwards at the speed of light whereas the maxima move at a speed around 15% less. Consequently, we are confident that the deviation of the speed of the maxima from 1 in Figs. 1 and 2 is not an artifact caused by the background energy density.

The work of L. Y. is supported by the U.S. Department of Energy under Grant No. DE-FG02-96ER40956. The work of P. C. is supported by a Pappalardo Fellowship in Physics at MIT. We are grateful to Scott Hughes, Paul Romatschke, and Ruben Rosales for useful discussions.

*pchesler@mit.edu
†lgy@uw.edu

[1] E. V. Shuryak, Nucl. Phys. **A750**, 64 (2005).
[2] J. M. Maldacena, Adv. Theor. Math. Phys. **2**, 231 (1998).
[3] E. Witten, Adv. Theor. Math. Phys. **2**, 253 (1998).
[4] J. L. Albacete, Y. V. Kovchegov, and A. Taliotis, J. High Energy Phys. 05 (2009) 060.
[5] Y. V. Kovchegov and S. Lin, J. High Energy Phys. 03 (2010) 057.
[6] S. S. Gubser, S. S. Pufu, and A. Yarom, J. High Energy Phys. 11 (2009) 050.
[7] S. Lin and E. Shuryak, Phys. Rev. D **79**, 124015 (2009).
[8] Y. V. Kovchegov and A. Taliotis, Phys. Rev. C **76**, 014905 (2007).
[9] D. Grumiller and P. Romatschke, J. High Energy Phys. 08 (2008) 027.
[10] G. Beuf, M. P. Heller, R. A. Janik, and R. Peschanski, J. High Energy Phys. 10 (2009) 043.
[11] R. A. Janik and R. B. Peschanski, Phys. Rev. D **73**, 045013 (2006).
[12] R. A. Janik and R. B. Peschanski, Phys. Rev. D **74**, 046007 (2006).
[13] S. de Haro, S. N. Solodukhin, and K. Skenderis, Commun. Math. Phys. **217**, 595 (2001).
[14] P. Anninos, G. Daues, J. Masso, E. Seidel, and W.-M. Suen, Phys. Rev. D **51**, 5562 (1995).
[15] R. M. Wald, *General Relativity* (Usa: Univ. Pr., Chicago, 1984), p. 491.
[16] J. P. Boyd, *Chebyshev And Fourier Spectral Methods* (Dover, New York, 2001), 2nd ed.
[17] S. Bhattacharyya, V. E. Hubeny, S. Minwalla, and M. Rangamani, J. High Energy Phys. 02 (2008) 045.
[18] R. Baier, P. Romatschke, D. T. Son, A. O. Starinets, and M. A. Stephanov, J. High Energy Phys. 04 (2008) 100.
[19] U. W. Heinz, AIP Conf. Proc. **739**, 163 (2004).
[20] P. M. Chesler and L. G. Yaffe, Phys. Rev. D **82**, 026006 (2010).